

Non-Gaussian Dark Matter perturbations and their imprint on the microwave background

Carlo Baccigalupi

INFN and Dipartimento di Fisica, Università di Ferrara, Via del Paradiso 12, 44100 Ferrara, Italy;
Osservatorio Astronomico di Roma, Viale del Parco Mellini 84, 00136 Roma, Italy
bacci@oarhp2.rm.astro.it

Abstract

The phases of the Fourier transform of any linear cosmological perturbation may be random (the Gaussian case) or not (the non-Gaussian case). If a non-Gaussian inhomogeneity was generated during the inflationary era by some process of very high energy physics, its evolution may be computed using the usual linear theory. I focus on the perturbations induced on the microwave background (CMB) by an underlying non-Gaussian distribution of dark matter (DM). Giving the specific example of an inflationary bubble, I show how non-Gaussian structures lying on the last scattering surface (LSS) may give rise to ordered patterns in the CMB anisotropy field. The next high resolution observations of the CMB sky may eventually detect these signals.

1 Introduction

Very high energy physics was dominant in the very hot phase of the universe. At $kT \simeq 10^{15}$ GeV the non-zero vacuum energy density of some fundamental field(s) may have driven a stage of accelerated expansion commonly known as inflation. This phase allows for the generation of perturbations in the cosmic density field, seeds of the structures we observe today, both in the DM distribution and in the cosmic radiation (see [7] for an extensive overview). Therefore, the accurate search for the observable traces of very high energy processes occurred in the early universe is very important to gain insight into domains inaccessible with accelerator physics.

In this contribute I focus on the CMB perturbations induced by such processes. The inflationary stage leaves traces in the form of Gaussian and/or non-Gaussian structures, described in general in Section II. In Section III I briefly recall how they are encoded in temperature perturbations and represent the seeds for the CMB anisotropies. Then, in Section IV, I point out that non-Gaussian DM inhomogeneities on the LSS may give rise to ordered patterns in the CMB anisotropy field; the usual CMB power spectrum, carrying the informations about the cosmological parameters, is not an appropriate tool for the detection of these signals. I give the specific example of the CMB anisotropy field caused by a DM inflationary bubble sitting on the LSS, showing how it could appear in the forthcoming Planck high resolution CMB maps.

2 Gaussianity and non-Gaussianity

At the end of the inflationary stage, the field(s) involved in the process decay in DM, baryons and radiation, leaving the cosmic density field $\rho(\mathbf{x}, t)$ perturbed around its mean value ρ by the traces of the perturbations generated during inflation: such traces are described through the density contrast $\delta\rho/\rho = \rho(\mathbf{x}, t)/\rho - 1$, well less than one if the perturbations are linear as assumed in all the cosmological theories. In order to distinguish between Gaussianity and non-Gaussianity, consider the Fourier transform of $\delta\rho/\rho$ written in the following way:

$$\left(\frac{\delta\rho}{\rho}\right)_{\mathbf{k}} = \left|\frac{\delta\rho}{\rho}\right|_{\mathbf{k}} \cdot e^{i\phi_{\mathbf{k}}} ; \quad (1)$$

depending on the properties of the phases $\phi_{\mathbf{k}}$, you can have the following distinction:

- **Gaussian perturbations:**

the phases $\phi_{\mathbf{k}}$ are random; $\langle \left|\frac{\delta\rho}{\rho}\right|_{\mathbf{k}}^2 \rangle$ describes completely the statistics ($\propto k$ in the simplest inflationary model). They are generated by the quantum fluctuations of the field driving the inflationary process during the slow rolling regime (see [7]).

- **non-Gaussian perturbations:** the phases $\phi_{\mathbf{k}}$ are not random, but reflect the shape of the fluctuation; the amplitude $\left|\frac{\delta\rho}{\rho}\right|_{\mathbf{k}}$ is generally strongly scale dependent (in most cases it involves only a finite set of wavenumbers \mathbf{k}). They are generated during inflationary phase transitions (defects [5], bubbles [6]).

3 Temperature perturbations

At the end of inflation the density field is perturbed in a generic way described in the previous section. This induces a corresponding perturbation in the temperature field $\delta T/T = T(\mathbf{x}, t)/T - 1$. Taking its Fourier transform, each Fourier mode evolve independently according to the linear theory; at decoupling ($_D$), the temperature inhomogeneities become anisotropies $(\delta T/T)(\theta, \phi)$ in the CMB sky. Summarizing, the process involves the following steps:

$$\frac{\delta\rho}{\rho}(\mathbf{k}, 0) \rightarrow \frac{\delta T}{T}(\mathbf{k}, 0) \rightarrow \text{evolution} \rightarrow \frac{\delta T}{T}(\mathbf{k}, t_D) \rightarrow \frac{\delta T}{T}(\theta, \phi) . \quad (2)$$

The temperature perturbations may be intuitively imagined as the addition of two components: a photon scattered at some point characterized by a temperature perturbation $(\delta T/T)_0$ carries the latter plus a Doppler component simply due to the

velocity of the baryon from which it was scattered, $(\delta T/T)_D$. These two quantities are governed by the following equations

$$\left(\frac{\delta \ddot{T}}{T}\right)_0 + 3\dot{\mathcal{R}}c_s^2\left(\frac{\delta \dot{T}}{T}\right)_0 + k^2c_s^2\left(\frac{\delta T}{T}\right)_0 = -\ddot{\Phi} - 3\dot{\mathcal{R}}c_s^2\dot{\Phi} - \frac{k^2}{3}\Psi \quad , \quad (3)$$

$$\left(\frac{\delta T}{T}\right)_D = -\frac{3}{k}\left[\left(\frac{\delta \dot{T}}{T}\right)_o + \dot{\Phi}\right] \quad , \quad \left(\frac{\delta T}{T}\right)_o(0) = \frac{-\Psi(0)}{2} \quad , \quad \left(\frac{\delta T}{T}\right)_D(0) = 0 \quad , \quad (4)$$

and we refer to [4] for a full treatment of them; here we only remark that the first one looks like a wave equation: c_s is the sound velocity of the system formed by baryons and photons, coupled by Thomson scattering. Also note that the system is driven by the gravitational potentials, that in Fourier transform are proportional to the density contrast:

$$\Phi, \Psi \propto \frac{\delta\rho}{\rho} \quad . \quad (5)$$

Finally, due to the same Thomson scattering, inhomogeneities are exponentially damped below the Silk damping scale. This is taken into account by multiplying each component of the perturbation by the factor $\exp[-k^2/k_D^2(t)]$, where the damping scale k_D^{-1} is of the order of ten comoving Mpc at decoupling.

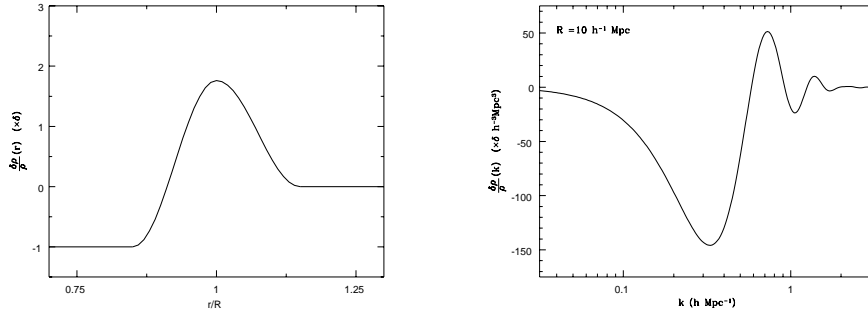


Fig.1 (left): bubble's density contrast radial profile. **Fig.2 (right):** its Fourier transform.

4 Perturbation evolution and CMB anisotropies

As I stated above, the primeval density perturbations may be Gaussian or not. In the first case, the CMB anisotropies resulting from the evolution of the system (3,4) are also Gaussian, and the CMB power spectrum completely describes the statistics. Instead, this is not true in the second case, that is the subject here.

A generic non-Gaussian perturbation is in general an ordered and spatially limited structure. Consider, just for example, a bubble in the density field at the end of inflation. Its density contrast may be easily analitically parameterized [1], and in figure 1 reports the radial density profile: the central cavity and the compensating shell are well visible; also note the linear scaling with the central density contrast

$\delta = (\delta\rho/\rho)_{r=0}$. Due to the spherical symmetry, the Fourier transform only depends on $k = |\mathbf{k}|$ and it is real if the frame center coincides with the center of the bubble, $\phi_{\mathbf{k}} = 0$ or π . Figure 2 reports the amplitude dependence on k . The comoving radius of the bubble is chosen to be $10 h^{-1}\text{Mpc}$ since it corresponds to the voids and structures observed today in the modern galaxy catalogues [3].

Each mode $(\delta\rho/\rho)_k$ is put as input in (5) of the gravitational potentials of the CMB equations at the end of inflation; the temperature perturbations evolve accordingly to the initial perturbation and to its own physics. At the end of the evolution all the k -modes are backtransformed to get the temperature perturbation in the real space:

$$\left(\frac{\delta T}{T}\right)_{\mathbf{x},t} = \int \frac{d\mathbf{k}}{(2\pi)^3} \left(\frac{\delta T}{T}\right)_{\mathbf{k},t} e^{i\mathbf{k}\cdot\mathbf{x}} . \quad (6)$$

The general phenomenology for an initial localized inhomogeneity is the following: the corresponding temperature perturbation propagates beyond the initial size, generating waves travelling outwards with the sound velocity c_s ; the signature of the underlying DM seed reaches the sound horizon at the time we are examining it. This is immediately evident by looking at figure 3. It represents the radial profile of $(\delta T/T)_0$ as it is at different times (redshifts), for a bubble with radius $R = 20 h^{-1}\text{Mpc}$. In panel *a* you can see the initial condition, that remain unchanged until the horizon reenter occurs (panel *b*); at this time a first central oscillation occurs, together with the origin of a positive crest. Soon after (panel *c*) a second opposite oscillation and the origin of a negative crest of the sound wave occur. Finally, the decoupling is reached with a central negative perturbation and a well visible outgoing sound wave (panel *d*).

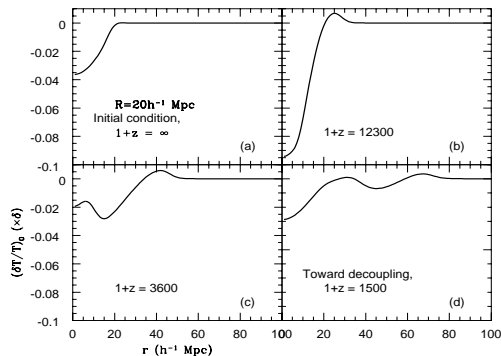


Fig.3: Time evolution of the temperature perturbation induced by a bubble.

At decoupling the above perturbations imprint anisotropies in the CMB sky in the following way. On a particular direction \mathbf{n} , the CMB anisotropy is given by

$$\left(\frac{\delta T}{T}\right)_{(\eta)_{\mathbf{n}}} = \int_0^{t_0} \left(\frac{\delta T}{T}\right)_{t,\mathbf{n}} P(t) dt , \quad (7)$$

where $P(t)$ is the probability for a photon to be last scattered between times t and $t + dt$. The perturbations examined here are spatially localized: they have a center

and are null beyond a sound horizon distance from it. Consequently, in performing the computation (7), we must specify the position of the perturbation with respect to the LSS. In the present case it is simply the distance d between the bubble's center and the LSS. Then the argument of the integral in (7) is

$$\left(\frac{\delta T}{T}\right)_{(\mathbf{n},d,t)} = \left[\left(\frac{\delta T}{T}\right)_0 + \left(\frac{\delta T}{T}\right)_{SW} + \left(\frac{\delta T}{T}\right)_D \cos \theta_{\mathbf{n}} \right]_{(\mathbf{n},d,t)}, \quad (8)$$

where the cosine of course accounts for the direction dependence of the Doppler effect and $(\delta T/T)_{SW}$ is the Sachs-Wolfe contribute given by the gravitational potential at the last scattering point (see [4]).

Figure 4 reports the CMB anisotropies from bubbles lying on the LSS; θ is the angle between the line of sight and the bubble's center direction. In each panel, three different lines show the variation of the angular dependence of $\delta T/T$ with the relative positions of the LSS with respect to the bubble's center: $d = 0, \pm 20 h^{-1}\text{Mpc}$; the central negative spots and the outgoing waves are well evident in both panels.

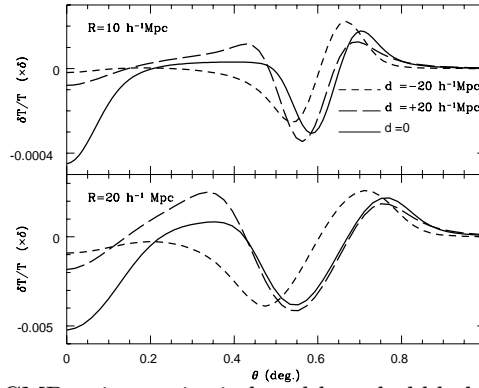


Fig.4: CMB anisotropies induced by a bubble lying on the LSS.

Finally look at figure 5, bottom panel; this is a portion of microwave sky in which a bubble with $R = 20 h^{-1}\text{Mpc}$ and $\delta = 10^{-2}$ lies exactly on the LSS ($d = 0$); the angular coordinates are in primes. In the general case, the non-Gaussian structures like the ones analyzed here are embedded in a Gaussian perturbation field filling the whole space [2]: then the figure reports the addition of the Gaussian CMB anisotropy plus the component given by the bubble. The circular imprint is well evident. Note that the DM bubble is in the central small dark spot, while the rings surrounding it are caused by the outgoing sound waves; consequently, the signal has the angular scales of the sound horizon at decoupling, that is nearly 1° in the sky. Just like a pebble in a pond, the initial small bubbly perturbation is propagating beyond the initial scale, reaching the scale of the sound horizon at the time in which we are examining it. In the upper panel, δ is half: in this case the Gaussian noise is quite dominant even if the underlying non-Gaussianity affects the statistics and may be searched with more sophisticated tools than the human eye.

If these structures are in a number sufficient to affect the structure formation,

they are expected to perturb the whole sky CMB power spectrum. In [2] we have analyzed in detail this case, showing that for a large number of possible statistics a distinctive peak at angular scales corresponding to $10'$ arises. This is not true for all the cases simply because when the statistics is not Gaussian the power spectrum does not fix univoquely the perturbation field. Thus, the ultimate imprint of the structures analyzed here has to be searched in higher order statistics.

Sub-degree full sky CMB maps shall be performed in the near future by the MAP and Planck experiments; they are consequently the most appropriate observations for the eventual detection of the signals treated here.

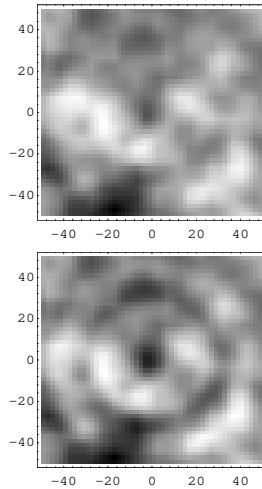


Fig.5: a portion of microwave sky generated by a bubble with $\delta = 10^{-2}$ (bottom) and $\delta = 5 \cdot 10^{-3}$ (top) lying on the LSS plus the standard Gaussian perturbations.

5 References

- [1] Baccigalupi C. 1998 *Ap.J.* **496** in press.
- [2] Amendola L., Baccigalupi C. & Occhionero F. 1998 *Ap.J.Lett.* **492** in press.
- [3] El-Ad H., Piran T. & da Costa L. N., 1997 *MNRAS* **287** 790.
- [4] Hu W. & Sugiyama N. 1995 *Ap.J.* **444**, 489
- [5] Pen U., Seljak U. & Turok N. 1997 *Phys.Rev.Lett.* **79**, 1611
- [6] Occhionero F. & Amendola L. 1994 *Phys.Rev.D* **50** 4846.
- [7] Padmanabhan T., Structure formation in the universe, *Cambridge university press* 1993.